Supplementary Materials

S1 Post-Processing Details

Voxel-wise calculations of the diffusion tensor were performed using an iteratively re-weighted linear least squares estimator,[1] in order to utilise information from both diffusion shells. From this, maps of FA and ADC were derived.[2] A representative 'response function' for white matter (WM), grey matter (GM), and cerebral spinal fluid (CSF) was then estimated, which provided the kernel for the deconvolution used in the CSD calculation. This was estimated using the '*dwi2response*' function in *MRtrix* after manually placing small ROIs (approx. 10 voxels) in each tissue type, using the b_0 and FA maps for guidance. Finally, voxel-wise estimation of the fODF was made using the MSMT-CSD technique,[3] with the maximum spherical harmonic order set to 8 for WM, and 0 for GM and CSF.

S1.1 Tractography

Tractography was performed using the WM fODFs, via a probabilistic streamlines algorithm.[4] The visual pathway was delineated in a piecewise manner in each patient, with the optic nerves, optic tracts, and optic radiations independently identified, on both the left- and right-hand sides of the brain. From each seed region (see below), 5000 streamlines were generated, with an fODF amplitude cut-off of 0.1 for terminating streamlines. The maximum angle between successive steps was set to 90° to allow for the high curvature of streamlines passing through Meyer's loop of the optic radiations.

The optic nerves were delineated by first placing a seed ROI at the intraocular segment of the optic nerve, identified using the b_0 image (Fig. S1a). Generating an initial set of 'unrestricted' streamlines from each eye allowed the optic chiasm to be identified (Fig. S1b). Whole brain sagittal and coronal exclusion planes were then placed to intersect with the centre of the chiasm, to separate the optic nerves on the left-/right-hand side, and restrict streamlines to the optic nerves only (Fig. S1c). Streamlines were then re-generated from the seed ROIs, to identify the left and right optic nerves (Fig. S1c). Stray streamlines passing through the extraocular muscles were manually excluded. An example of optic nerve tractography in a patient with tumour invasion of the optic nerve is shown in Fig. S1d-f.

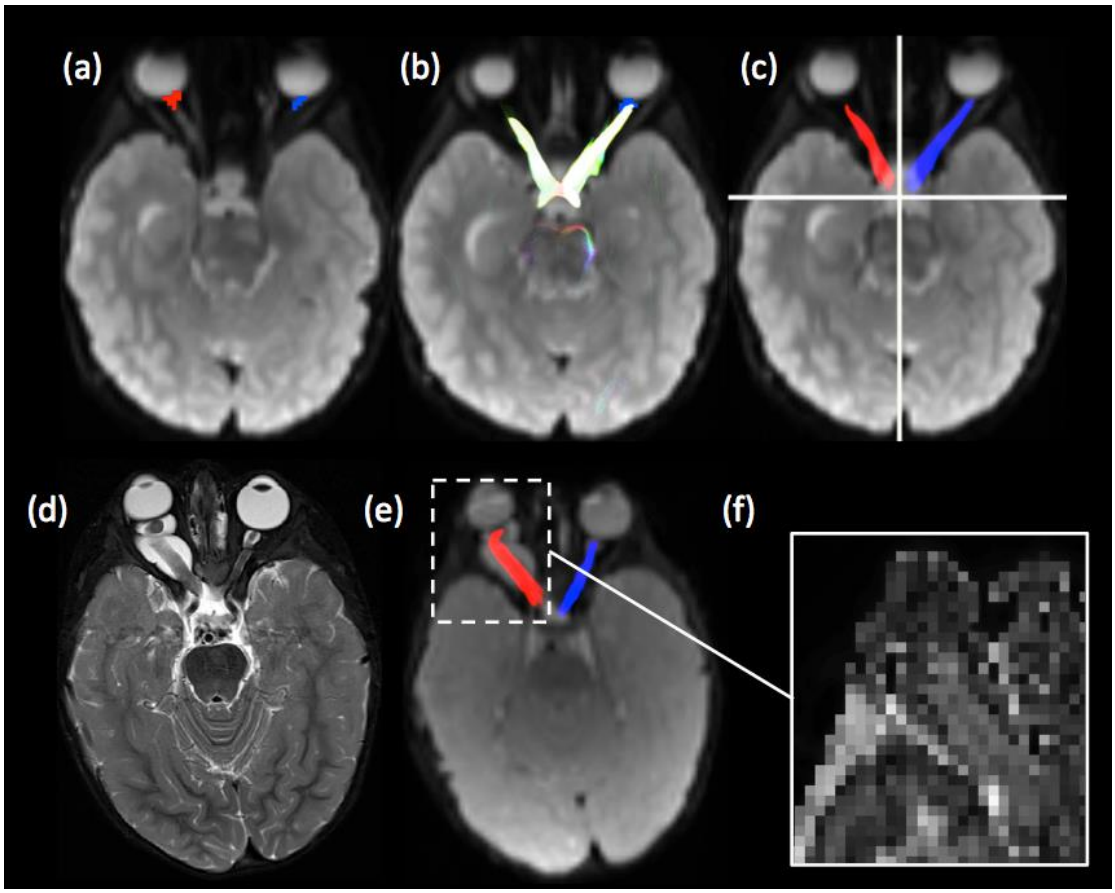

Figure S1 *Top row: Delineation of the optic nerves. (a) Axial b_0 image, with right (red) and left (blue) seed ROIs at the junction between the optic nerve and eyeball. (b) Initial, 'unrestricted' streamlines from the seed ROIs. (c) Placement of sagittal*

and coronal exclusion planes (white lines), and final tracts representing the right (red) and left (blue) optic nerves. Bottom row: Example of optic nerve tractography in the presence of tumour infiltration. An axial slice from the clinical T2w sequence is shown in (d), with significant tumour invasion of the right optic nerve. (e) Streamlines representing the right and left optic nerves overlaid on the b_0 image, in approximately the same location. (f) Enlarged section of the FA map, showing the region indicated by the white box in (e).

Seed ROIs for the optic tracts were placed immediately posterior to the coronal exclude plane, over the anterior-posterior orientated fibres which appear as green coloured regions on the colour-FA map (Fig. S2a). Again, an initial set of 'unrestricted' streamlines from these ROIs was generated (Fig S2b). Stray fibres passing into the anterior commissure and optic radiations were manually excluded (Fig S2b, green arrows). Additionally, an axial exclude plane was placed superior to the optic tracts to exclude streamlines passing into the cortico-spinal tracts (Fig S2c). The sagittal and coronal exclusion planes defined above were also used, to differentiate the left/right optic tracts, and to prevent streamlines travelling back into the optic nerves, respectively. With these exclude regions in place, the streamlines were re-generated from the initial seed ROIs to delineate the left and right optic tracts (Fig S2d).

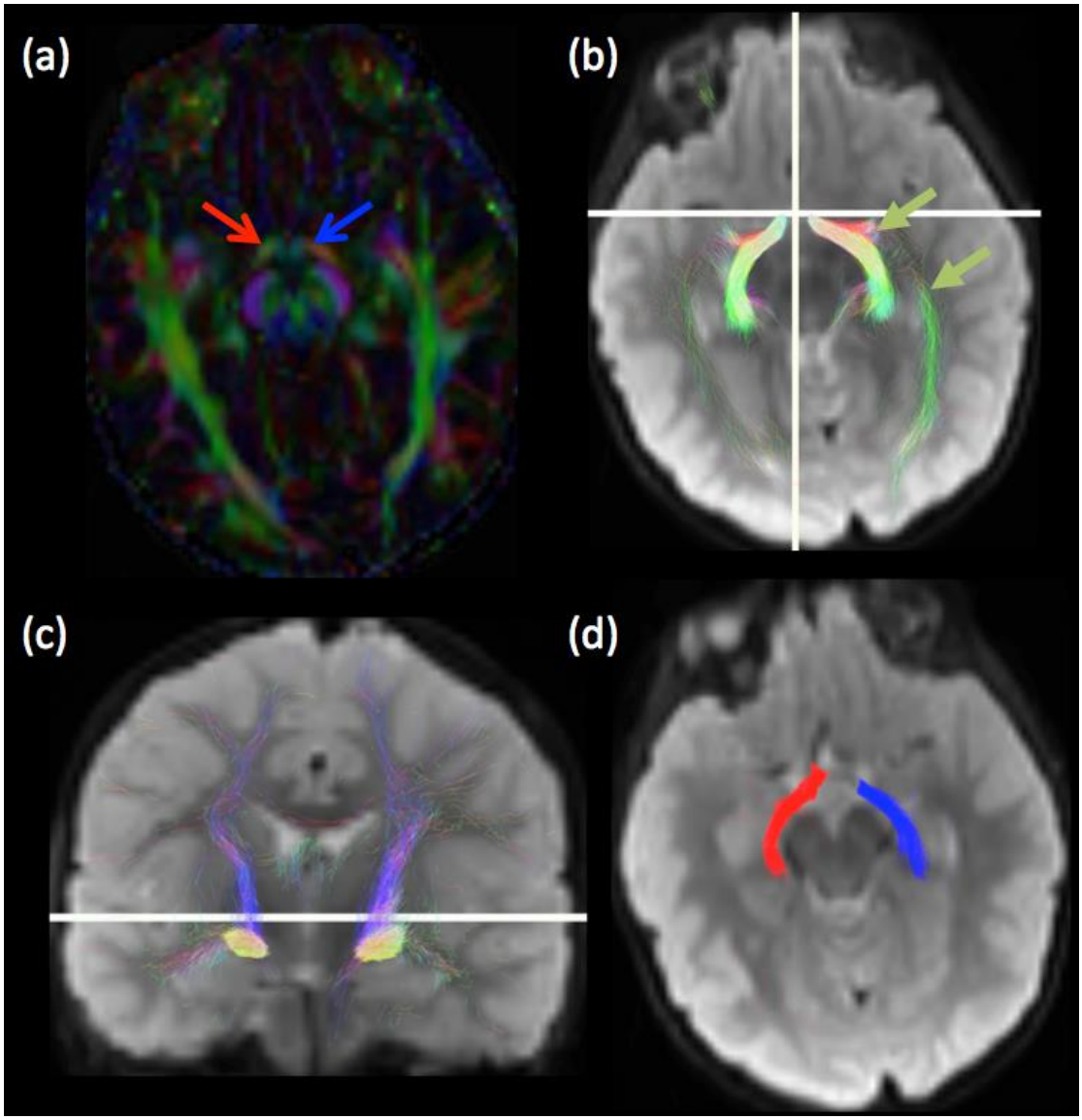

Figure S2 *Delineation of the optic tracts in a representative patient. (a) Axial colour-coded FA map, in which anterior-posterior orientated fibres are shown in green, left-right orientated fibres in red, and superior-inferior orientated fibres in blue. Brightness is modulated by FA value. The location of seed ROIs for the right (red arrow) and left (blue arrow) optic tracts are overlaid. (b) Initial, 'unrestricted' streamlines from the ROIs shown in (a), after which sagittal and coronal exclusion planes were overlaid (white lines). Green arrows indicate stray streamlines passing into the anterior commissure and optic radiations, which were manually excluded. (c) Coronal view indicating placement of the additional axial exclude plane (white line) to exclude streamlines passing into the cortico-spinal tracts. (d) The final streamlines representing the right (red) and left (blue) optic tracts.*

The optic radiations were identified by placing a seed ROI near the lateral geniculate nucleus (LGN). This was identified using a coronal slice, as an isolated

region of anterior-posterior orientated fibres (green on the colour-FA map, Fig S3a). The location of this coronal slice was chosen to coincide approximately with the termination of the optic tracts identified in the previous step. A waypoint was placed over the anterior-posterior orientated fibres located laterally to the lateral ventricles and posterior to the LGN (Fig S3b). The sagittal and coronal exclusion planes used in the previous two steps were also used, allowing delineation of the left and right optic radiations (Fig S3c). Stray streamlines passing into the splenium of the corpus callosum were manually excluded.

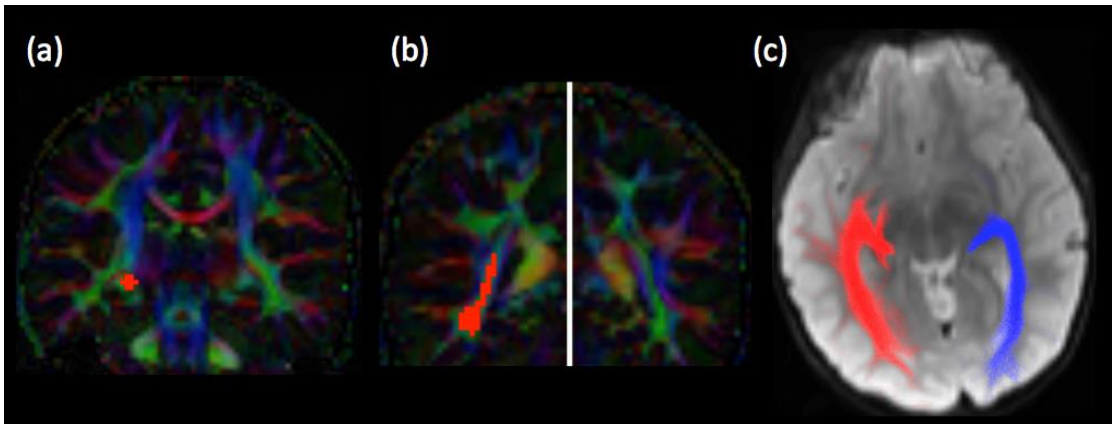

Figure S3 *Delineation of the optic radiations in a representative patient. (a) Coronal colour-coded FA map, with the seed ROI for the right optic radiation overlaid in red. (b) Placement of the waypoint for the right optic radiation (red ROI), over anterior-posterior orientated fibres located laterally to the right-lateral ventricle. The sagittal exclude plane is indicated by the white line. (c) The final streamlines representing the right (red) and left (blue) optic radiations.*

The final white matter tracts were converted into track density images in the native space of the diffusion scan, using *tckmap* in *MRtrix*. Voxels containing less than 5% of the generated streamlines for each tract were excluded to remove stray streamlines, and a binary mask was created for the remaining voxels, to provide ROIs defining the location of optic nerves, tracts, and radiations in each patient. Median values of FA and ADC were then measured in each ROI.

S1.2 Tumour ROI co-registration

In order to compare the tumour locations across the cohort, a group-wise registration was performed using *NiftyReg* software (Centre of Medical Image Computing, University College London). Here, the mean-FA map across the cohort was used as the initial target image, and each patient's individual FA map was affine registered to this. A new mean-FA map was then produced from the co-registered FA maps, and each patient's original FA map was then registered to this. This affine transformation was then applied to each patient's tumour ROI, to bring all tumour ROIs into the mean-FA space.

S2 References

1. Veraart J, Sijbers J, Sunaert S, Leemans A, Jeurissen B. Weighted linear least squares estimation of diffusion MRI parameters: strengths, limitations, and pitfalls. *NeuroImage*. 2013;81:335-346. doi:10.1016/j.neuroimage.2013.05.028.

2. Basser PJ, Pierpaoli C. Microstructural and physiological features of tissues elucidated by quantitative-diffusion-tensor MRI. *J Magn Reson B*. 1996;111(3):209-219.

3. Tournier J-D, Calamante F, Gadian DG, Connelly A. Direct estimation of the fiber orientation density function from diffusion-weighted MRI data using spherical deconvolution. *NeuroImage*. 2004;23(3):1176-1185. doi:10.1016/j.neuroimage.2004.07.037.

4. Tournier J-D, Calamante F, Connelly A. MRtrix: Diffusion tractography in crossing fiber regions. *Int J Imaging Syst Technol*. 2012;22(1):53-66. doi:10.1002/ima.22005.